ACCELERATED AGING AND DURABILITY OF COMPOSITE RODS FOR POWER TRANSMISSION LINES

N.K. Kar[a], Y.-I. Tsai[a], E. Barjasteh[a], E.J. Bosze[a,b], S.R. Nutt[a]
[a]University of Southern California, Composites Center
Vivian Hall of Engineering, Los Angeles, CA 90089
[b]Composite Technology Corporation
2026 McGaw Ave., Irvine, CA 92614
nkar@usc.edu
boldlike@hotmail.com
barjasteh.ehsan@gmail.com
ebosze@compositetechcorp.com
nutt@usc.edu

SUMMARY

A pultruded glass fiber/carbon fiber composite rod has been developed to support overhead transmission lines. The rod is wrapped with aluminum strands to produce the conductor. When compared with conventional steel-reinforced conductors in use today, the composite conductor can support more aluminum, operate at higher temperatures with lower sag, and exhibits 1.5 times the tensile strength.

Keywords: Glass fiber, carbon fiber, epoxy, conductor, accelerated aging

ABSTRACT

Transmission lines typically consist of electrically conductive Al wires that are supported by a stranded steel cable core, and the lines are hung from lattice towers. Figure 1 shows a section of conventional ACSR overhead conductor (aluminum conductor/steel reinforced). Despite widespread use, ACSR lines have inherent limitations, one of which is the high CTE (coefficient of thermal expansion) values of the aluminum and steel wires (23 and 11.5×10^{-6}/°C). When amperages increase and the line temperature rises, linear expansion causes substantial sag between towers. The extent of sag limits the operating temperature (because safety dictates that minimum clearances be maintained), and ultimately the distribution capacity of the electrical grid. Although the design of transmission lines has not changed substantially in the past 100 years, new designs have appeared in recent years. In one such design, the stranded steel core is replaced with a solid composite rod of unidirectional glass and carbon in epoxy, as shown in Figure 1. The advantages of the composite conductor (ACCC, aluminum conductor/composite core) include a low CTE value (nearly an order of magnitude less than steel), strength that is nearly 1.5 times the steel wire used in ACSR conductor (2158 MPa vs. 1240 MPa), and a density roughly 1.3 that of steel [1]. The lower CTE value results in greatly reduced sag at high service temperatures [1]. In terms of electrical performance, the ACCC cable has a higher electricity transmission capacity

(ampacity), because (1) the round Al wires are replaced with trapezoidal wires, filling interstitial spaces, and (2) the operating temperatures can be well over 100°C because the sag is nearly eliminated by the low-expansion composite core.

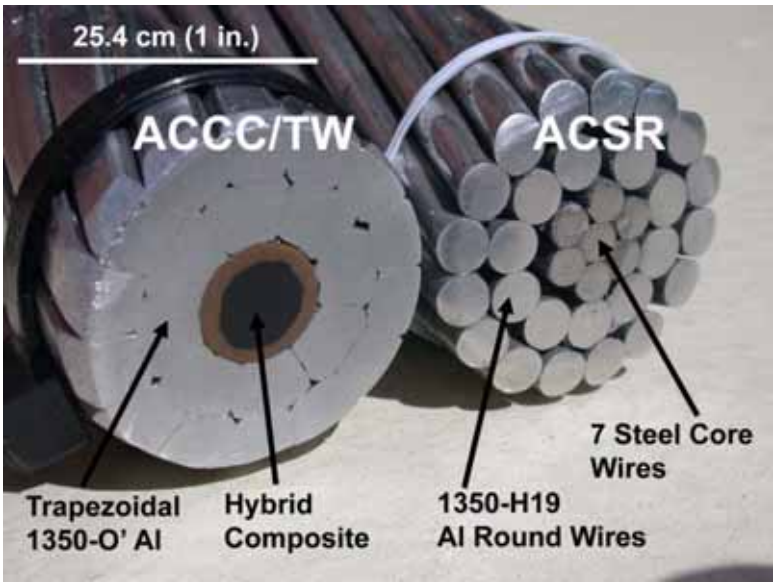

Figure 1. The Composite core conductor (ACCC, left) and the conventional steel-reinforced conductor (ACSR) commonly used today.

The ACCC conductor is intended for sustained operation up to 180°C. Thus, the long-term durability of the composite core is a key performance issue, and the effects of thermal exposure (25°C-200°C), moisture, and cyclic loads on tensile strength have been investigated [2]. Retention of tensile strength is critical, since the core supports nearly all of the mechanical loads. The effects of accelerated aging on strength, glass transition temperature, and microstructure has been investigated. Water uptake and thermal oxidation experiments have shown that while both processes can lead to strength degradation, the service conditions anticipated for the composite are more moderate, and lifetimes are expected to be more than adequate [3]. This report will focus on accelerated aging experiments and degradation mechanisms, as well as the implications for long-term durability.

INTRODUCTION

The effort to develop a pultruded glass/carbon composite rod for use in overhead conductors requires an understanding of the effect of environmental exposure on long-term retention of bulk material properties. For overhead conductors, environmental attack results primarily from exposure to temperatures, moisture, radiation, aggressive chemicals, and combinations of these factors with mechanical loads. These factors can (and generally do) affect the mechanical and physical properties of composites in adverse ways, as described in multiple studies [4-9]. The service life of overhead conductors can span several decades, with an expectation of little or no maintenance. To design for such service life requires the ability to forecast changes in material properties as a function of environmental exposure.

Moisture in any form is potentially problematic for polymer composites, as it often causes swelling and degradation. Matrix and/or interface degradation resulting from moisture absorption is a particular concern for overhead conductors, which are subject to atmospheric conditions ranging from precipitation to mild humidity over a wide temperature range. Complete immersion in water constitutes the most severe environment, while humid air generally results in lower maximum moisture content [10-12]. Long-term exposure at high temperatures can accelerate diffusion rates of moisture and generally accelerate aging. Various aspects of moisture-induced behavior and the dependence on such factors have been studied, and both Fickian and non-Fickian diffusion behavior have been reported [6-9, 12, 13-17]. We have undertaken studies to assess the hygrothermal effect on moisture content, short beam shear strength, and glass transition temperature (T_g) for the pultruded glass/carbon composite rod.

At high temperatures (approaching the glass transition temperature T_g), polymer composites are susceptible to oxidative degradation [18-21]. Although the fibers are stable at such temperatures (less than T_g), the matrix and especially the fiber-matrix interface can undergo degradation that affects the physical and mechanical properties of the structure over time. Matrix oxidation of composites has been investigated for polymers such as polybismaleimide [22, 23] and amine cured epoxy [24-26]. The oxidation is initially limited to a superficial layer until cracks first appear in the layer. Cracks open new pathways for oxygen to penetrate the specimen and lead to more extensive oxidation. This process can continue until the polymer is completely oxidized. During oxidation, polymers undergo mass loss, shrinkage, and increased density [27].

Spontaneous cracks due to the matrix oxidation initiate and propagate within the oxidized layer at the surface of the structure [28]. Therefore, prediction of the thickness of the oxidized layer, TOL, helps to design more efficient and durable structures and hence to prevent as much damage as possible. We have performed experiments to determine kinetics of thermal oxidation and associated damage mechanisms for a pultruded glass/carbon composite rod designed to support overhead conductors. A coupled reaction-diffusion model was developed for the carbon fiber (CF) core and the glass fiber (GF) shell to predict the oxygen concentration profile and the TOL. The effect of oxidation on tensile strength and also crack initiation and propagation in the hybrid composite was analyzed [29].

EXPERIMENTAL PROCEDURE

Materials

The material used in this study was a pultruded hybrid composite rod (Composites Technology Corporation, Irvine, California). The rods were 9.53 mm in diameter and comprised of a carbon fiber (CF) core surrounded by a glass fiber (GF) shell as shown in Figure 2. The epoxy matrix was formulated to achieve a high glass transition temperature (T_g) using a propriety epoxy recipe and an anhydride curing agent. The rod characteristics are shown in Table 1.

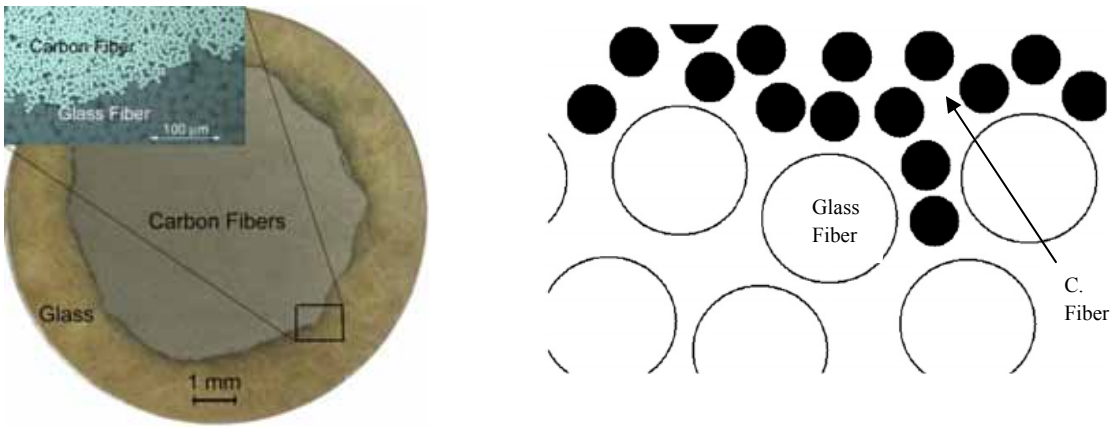

Figure 2. A cross sectional view of the composite rod, showing the carbon fiber core and glass fiber shell.

Table 1. Characteristics of carbon fiber core and glass fiber shell in composite rod.

	r_i (mm)	r_o(mm)	% glass volume	% carbon volume	% epoxy volume	% cross sectional area
Carbon core	0	6.8	0	69	31	51
Glass shell	6.8	9.5	64	0	36	49

Conditioning for Moisture Uptake Experiment

In addition to the 9.53 mm diameter hybrid composite rods, control samples comprised of all-CF and all-GF composite 6.3 mm diameter rods were produced as the control group to compare diffusion coefficients and behavior. All samples were cut to a length of 66.5 mm using a diamond saw and a silicone sealant was applied to the specimen ends to prevent moisture penetration on the cut ends. Prior to water immersion, all the specimens were dried in a 100°C oven for 2 days to remove the retained moisture during the storage. All samples were then weighed by using an analytical balance (ACCULAB LA-60) with 0.001 mg accuracy. The specimens were then placed in a large Pyrex dish containing de-ionized water at 40°, 60° and 90°C, separated by wire mesh to avoid specimen contact. Samples were removed from the baths at predetermined times up to 32 weeks. All samples were subsequently weighed to determine weight change. The weight gain was calculated according to:

$$\frac{W_w - W_o}{W_o} \times 100\%, \qquad (1)$$

where W_w is the wet weight and W_o is the dry weight. After weighing, the specimens were divided into two groups of three samples each. The first group was not dried, and the short beam shear (SBS) strength and T_g was determined in the ‘‘wet” state. The second group of samples was dried in a 100°C oven for 2 days to stabilize the weight, and then the same measurements were performed. Drying the second set of samples was performed to determine if any decrease in property values was reversible by removing the absorbed moisture.

Conditioning for Oxidation Experiment

In addition to the 9.53 mm diameter hybrid composite rods, control samples were produced by a clear casting method that involved curing the neat resin for one hour at 200°C. Samples were placed in an air-circulated oven at 180°C and 200°C and 1 atmosphere pressure for isothermal aging. Samples were separated to allow convection, and sample ends were capped with a silicone sealant to prevent end-diffusion of oxygen on the cut ends. All samples were then weighed by using an analytical balance (ACCULAB LA-60) with 0.001 mg accuracy. Samples were cooled in a desiccator for 10 minutes before every measurement to prevent moisture adsorption. The same procedure was used for clear cast samples to record weight loss.

Mechanical Testing and Thermal Analysis

The influence of hygrothermal exposure on mechanical and thermal properties of the composite rods was studied. After exposure, SBS strength was measured in accordance with ASTM D4475-02 using a span length 6 times the diameter and a crosshead displacement rate of 1.3mm/min (INSTRON 5567). Dynamic mechanical analysis (DMA) was performed to determine the shift of T_g in accordance with standard protocol (ASTM D7028). A dual cantilever beam clamp was employed using a commercial instrument (TA Instruments, DMA 2980). Rectangular samples (60 × 9.5 × 1.6 mm) were sectioned from the CF core of the rod, and the T_g was determined from the peak in the loss modulus curve. Transverse sections were cut and polished, then examined microscopically to determine if cracking occurred with different exposure times. In addition, dye penetrant was used to detect cracks in the aged samples.

The influence of oxidative environment on the mechanical and thermal properties was also studied. DMA was performed to determine the shift of T_g for oxidized composite rods and the neat epoxy. The tensile strength of the composite core was measured using a computer controlled load frame (INSTRON 5585) following ASTM D3916. Tensile tests were performed by preloading the samples to 4.5 kN and holding for 5 minutes to allow load redistribution in the load train. All tests were conducted at 20°C, and the load was applied at a constant crosshead speed of 5mm/min until failure occurred. Polished sections were examined to measure the oxidized thickness and to detect cracks.

RESULTS

Moisture Uptake

The moisture absorption behavior is shown in Figure 3, where the percent weight gain is plotted as a function of the square root of immersion time ($s^{1/2}$) at each temperature. Each point represents the average of measurements on six specimens, and the error bar is the standard deviation. The weight gain values for the 40°, 60° and 90°C baths after 5300 hours (32 weeks) were 0.53 ± 0.03%, 0.90 ± 0.04% and 11.74 ± 1.22% respectively. The solid lines are the Fickian diffusion curves obtained by plotting the theoretical equation [30]:

$$M_t = \left[1 - \sum_{n=1}^{\infty} \frac{4}{a^2 \alpha_n^2} \exp\left(-D\,\alpha_n^2\, t\right)\right] M_\infty \qquad (2)$$

The saturation level of water absorption, M_∞, is assumed to be constant for complete immersion in water [10] if cracking does not take place. The diffusion coefficient is D, the radius of the composite rod is a, and α_n is the n^{th} root of the zero-order Bessel function. The cylindrical geometry of the rod dictates the use of the Bessel function, and because samples were capped on the ends with sealant, diffusion took place only in the radial direction. The diffusion coefficients in Table 2 were determined by fitting the initial slope of Eq. (2) and choosing 1% as the assumed saturation point. Below the saturation point, moisture absorption was responsible for the weight gain, while above the saturation point, the development of cracks led to a large increase in weight because of the entrapment of infiltrated moisture [3].

The moisture absorption mechanism of the hybrid GF/CF composite rod was considered [3]. Figure 3 indicated that the weight gain data for samples at 40°, 60° and 90°C coincided with Fickian curves for the first 1344 hours (~2200 $s^{1/2}$), 1000 hours (~1900 $s^{1/2}$) and 625 hours (~1500 $s^{1/2}$) respectively. Non-Fickian behavior was observed in 40° and 60°C samples prior to saturation. To determine if the CF/GF interface was involved, all-CF and all-GF composite rods were also exposed to 60°C water. These rods were smaller than the hybrid GF/CF composite (6.3 versus 9.53 mm), and had higher fiber loadings (75% versus 70%). Because of the slightly higher fiber loadings, the rods saturated to a lower moisture level (0.85% versus 1%), but note that the absorption curves in Figure 4 show no evidence of a change in diffusion rate before saturation. The distinctly different behavior of the hybrid composites was attributed to the presence of the radial GF/CF interface, shown in Figure 2 [3].

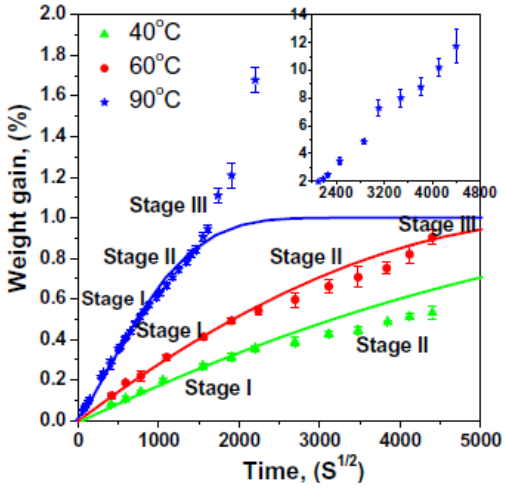

Figure 3. Weight gain versus the square root of time for hybrid composites immersed in 40°, 60°, and 90°C water.

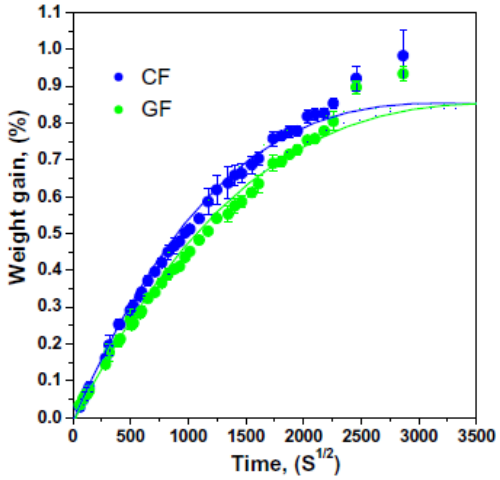

Figure 4. Weight gain versus the square root of time for control composites immersed in 60°C water.

Table 2. Initial diffusivity coefficients for each water immersion experiment

Temperature (°C)	40	60	90
$D(m^2s^{-1})$	1.42×10^{-13}	3.84×10^{-13}	2.7×10^{-13}

As the amount of water absorbed by the composite increased with time, reductions in T_g and SBS strength were measured. Hygrothermal exposure strongly affected the rate at which T_g decreased. For weight gains of 0.5% the T_g values were 165°, 175° and 190°C for immersion in water at 40°, 60° and 90°C. The increase in T_g with immersion temperature stems from the fact that higher exposure temperatures produced steeper concentration profiles, resulting in smaller decrements in T_g [3]. The reduction and retention of thermal and mechanical properties are shown in Table 3. Samples exposed to 40° and 60°C for 32 weeks showed 85-98% recovery in SBS strength and 77-91% recovery of T_g. Samples exposed at 90°C for 4 weeks also showed comparable retention. In summary, removal of moisture resulted in nearly full recovery of both T_g and SBS, while the moisture level was below the saturation point. Once the saturation point was exceeded, these properties did not recover and exposure caused permanent damage to the matrix through crack formation. The unusually high moisture content in the 90°C samples is tentatively attributed to moisture entrapment in cracks, although this assertion awaits further investigation.

Table 3. Reduction (Red.) and retention (Ret.) of thermal and mechanical properties.

	Shear Strength (MPa)	Red./Ret. (%)	T_g(°C)	Red./Ret. (%)
Start	48	0	209	0
40°C (32 wks)	41.8/47.2	87/98	160.3/189.5	77/91
60°C (32 wks)	38.2/40.7	80/85	146/160.2	70/77
90°C (4 wks)	37/41.8	77/87	153.5/168.4	73/81

Oxidation Exposure

The oxidation exposure behavior of the hybrid composite rods is shown in Figure 5. Weight loss is plotted as a function of time for two temperatures, 180° and 200°C. The weight loss increased with exposure temperature and the rate of weight loss was high for the first 10-20 hours, and then reached a steady state for the duration of the aging. The total weight change of the hybrid composite is expressed in equation (3) [31].

$$(1-w_f)\frac{1}{m_0}\frac{dm}{dt}=\frac{32}{\rho_0}r(C)-\frac{18}{\rho_0}\frac{d[H_2O]}{dt}-\frac{M_v}{\rho_0}\frac{d[V]}{dt}-\mu_0 \qquad (3)$$

Where w_f, M_v, m, ρ_0 and μ_o are the mass fraction of fibers, average molar mass of volatile fragments, the mass of the specimen, initial density, and the volatile emission in the absence of oxygen, respectively. The weight loss resulted from (a) the loss of volatiles, (V and μ_0), (b) inherent water evaporation and (c) weight gain associated with the oxidation reaction. Each term on the right-hand side of equation (3) can be expressed in terms of oxygen concentration using kinetic equations, leading to a final equation relating mass loss to oxygen concentration [22].

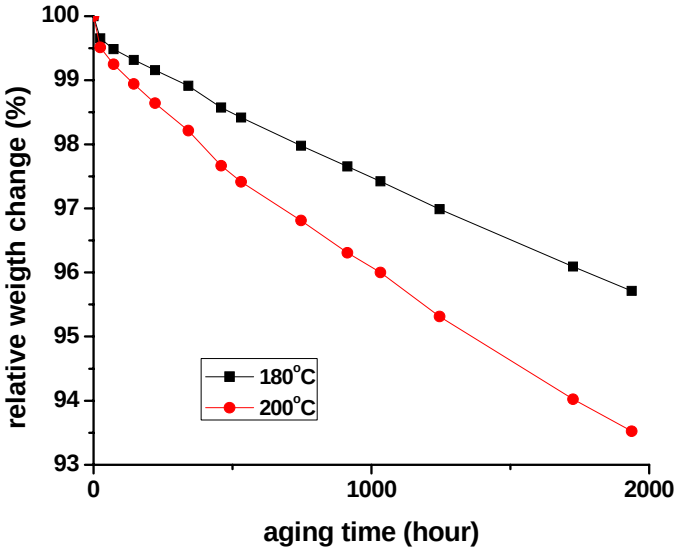

Figure 5. The gravimetric curve obtained for 30.48 mm in length and 9.53 mm in diameter capped composite rods thermally aged at 180°C and 200°C.

After required phenomenological parameters were determined [31], two coupled non-linear differential equations (4, 5) were solved numerically by applying boundary and initial conditions as shown below. The solution predicted oxygen concentration profiles within the carbon core, $C_c(r, t)$, and within the glass shell, $C_g(r, t)$.

$$\frac{\partial C_c}{\partial t} = D_{carbon/epoxy}\left(\frac{\partial^2 C_c}{\partial r^2} + \frac{1}{r}\frac{\partial C_c}{\partial r}\right) - r_1(C_c) \tag{4}$$

$$\frac{\partial C_g}{\partial t} = D_{glass/epoxy}\left(\frac{\partial^2 C_g}{\partial r^2} + \frac{1}{r}\frac{\partial C_g}{\partial r}\right) - r_2(C_g) \tag{5}$$

Boundary Conditions: (6)

$$r = R_o \qquad C_g = C_s$$

$$r = R_c \qquad C_g = C_c \qquad \frac{\partial C_c}{\partial t} = \frac{\partial C_g}{\partial t}$$

$$r = 0 \qquad \frac{\partial C_c}{\partial t} = 0$$

In equations 4 and 5, $D_{glass/epoxy}$ and $D_{carbon/epoxy}$ are the diffusivities of oxygen through the glass shell and carbon core, respectively. In these expressions, $r_1(C_c)$ and $r_2(C_g)$ are the reaction rates of oxygen within the glass shell and the carbon core, respectively. Initially, C=0 for all points in the rod, and C_s is the concentration of oxygen at the surface of the rod. Boundary conditions at $r = R_c$ are defined assuming a continuous oxygen concentration at the CF-GF core-shell interface. The matrix material in both components is a cyclo-aliphatic epoxy. However, the diffusion coefficients are not

identical for the two sections. The difference stems from multiple factors, including the fact that the difference in the fiber volume fractions is not the same in the two sections, nor is the path length (tortuosity) [32, 33]. In particular, the tortuosity, which is inversely related to diffusivity, differed in the two sections because of the different diameters of CF and GF fibers [3].

Figure 6 shows the predicted oxygen concentration profiles as a function of radial position within the hybrid composite for different aging times. The predicted oxygen concentration decreased with increasing depth in the GF shell, as expected, and approached zero at depths of 25-150 μm, depending on aging time. Note that the concentration profiles were essentially the same for aging times of 672 and 100 hours. The prediction is accurate for long aging times, (to be shown below), unless the composite surface undergoes severe damage, such as surface erosion or cracking.

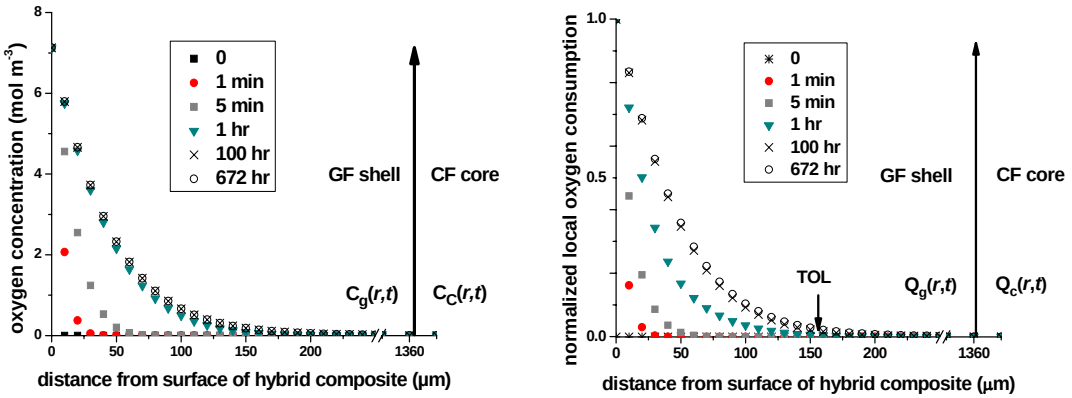

Figure 6. Simulation prediction of oxygen concentration profiles for hybrid composite rods ,$C_c(r, t)$, and $C_g(r, t)$, in air at 180°C.

One can calculate the local oxygen consumption at a particular radial position by integrating the local oxygen consumption rate over aging time, $Q = \int_0^t r(c)dt$ [29]. The calculated values can be used to plot the normalized oxygen consumption as a function of radial position within the hybrid composite. Such a plot is shown in Figure 6 for different aging times. The plot indicates the amount of epoxy converted to oxidation product (conversion degree of oxidation). The oxygen consumption decreased with increasing subsurface depth and asymptotically approached zero, because of the shortage of oxygen molecules arising from the oxygen concentration gradient. Thus, the oxidation thickness for different exposure times can be determined from the plot by simply reading the points at which the conversion degree is approximately zero. The oxidation concentration profiles and associated reaction products formed relatively quickly (<100 h), and thicknesses (TOL values) reached a limiting value of ~155 μm. The TOL remained essentially constant after 100 hours, even for isothermal exposures up to one year.

The oxidation thickness was also measured by oxidizing rods (30.5 mm long) at 180º and 200ºC. Polished cross sections of aged composite rods were inspected to measure the oxidization thickness (TOL), as shown in Figure 7. The oxidation was limited to two discrete superficial layers within the GF shell. The outermost layer underwent more

extensive oxidation, and was assumed to correspond to a 50% conversion of the matrix (see Figure 6) [19]. The subsurface layer (Y), was less extensively oxidized, and the combined thickness of the two layers constituted the total oxidation layer of the composite, or TOLC. Aging at 200°C produced a TOLC comprised of a single layer (two distinct layers were not detected). The measured TOLC values for both aging exposure temperatures are tabulated in Table 4, along with model-based predictions. The thickness values were determined from the average of 20 thickness measurements at each temperature. Comparison of the measured and predicted TOLC values reveals a difference of roughly 6%, both at 180°C and 200°C. Note that no evidence of oxidation was detected within the CF core, which is consistent with the prediction.

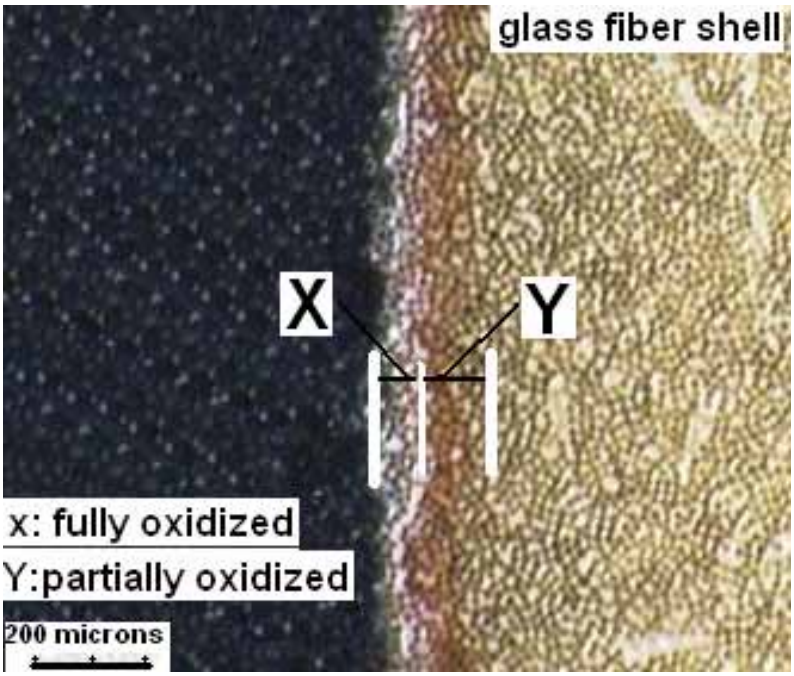

Figure 1. Transverse cross section of hybrid composite rod thermally aged in air at 180°C for 672h. The TOLC is confined to a thin layer at the surface.

Table 4. Comparison of measured TOLC (oxidation thickness) with predicted values, for aging exposures at 180°C and 200°C in air for 672h.

Aging Temperature	Predicted TOLC (μm)	Measured TOLC (μm)
180°C	155	146 ± 18
200°C	110	117 ± 5

Predictions of the TOLC can be extended to longer aging times using the model presented in equations (4) and (5). Inspection of oxidized composites aged for 8,736 hours at 180° and 200°C showed no significant changed in TOLC. This is illustrated in Figure 8, which shows the measured and predicted TOLC values for thermal exposure at 180°C. The plot also shows the predicted TOLC value of 155 μm, which is similar to the measured TOLC (~140 um). (Note that 180°C is the maximum anticipated service temperature for the overhead conductors). No evidence of crack formation was detected

for aged samples up to 8,736 hours, and the tensile strength of the composite rod remained unchanged after thermal oxidation.

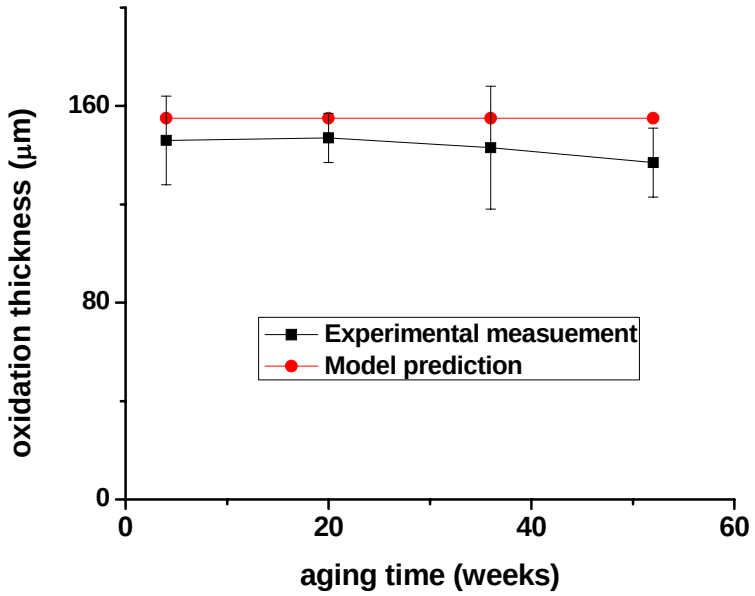

Figure 2. Measured TOLC for aging times up to 52 weeks at 180°C.

DISCUSSION

The hybrid composite featured a GF shell intended primarily to prevent galvanic coupling between the CF core and the overlaid aluminum wires of the conductor [1, 34]. This had two additional effects. First, this created a GF/CF interface, which affected diffusion behavior by acting as a temporary moisture barrier when exposed to a severe hygrothermal environment. Secondly, the GF shell underwent severe oxidation during initial exposure, forming a scale that acted as a barrier against oxidation, limiting oxidative damage to a few fiber diameters.

The anticipated service temperature range for overhead conductors is 50-180°C. Consequently, the moisture concentration within the composite rods should never reach a saturation point in service conditions. Samples immersed at 40° and 60°C did not reach saturation in the 32-week exposure period, and two stages of moisture absorption of primary interest were identified. Stage I followed a theoretical Fickian curve, as diffusion kinetics are determined by the GF shell. The stage ended when the moisture content in the shell reached a critical value where the diffusion rate changed. For exposures at 40° and 60°C, the slope of the weight gain changed at 2200 and 1900 $s^{1/2}$, signaling the end of Stage I. The GF/CF interface played an important role as a moisture barrier, altering the diffusion mechanism in Stage II. In this stage, the diffusion rate decreased due to the inhomogeneity of the GF/CF interface. After 32 weeks, the 40° and 60°C samples were still in Stage II as seen in Figure 2.

The change in the diffusion rate between Stages I and II was associated with denser fiber packing at the GF/CF interface. Closer examination of the GF/CF interface revealed intermingling of the CF with the larger GF, where the smaller CFs slipped into

interstitial sites between larger GFs, as shown in Figure 2. Image analysis using the linear intercept method revealed that fiber loadings of the core and shell regions were 67%, but the local fiber loading at the GF/CF interface was 75%. The closer packing at the annular interface retards the diffusion of moisture, and acts as an effective moisture barrier.

Degradation resulting from hygrothermal exposure is often caused by damage to the fiber/matrix interface, and generally results in a decrease in strength and modulus [15]. Moisture absorption also softens the matrix, degrading the stress transfer function and resulting in a substantial loss of T_g and SBS strength. In the present study, the removal of absorbed moisture led to significant recovery (77-98% of original values) for thermal and mechanical properties, although full recovery was not achieved, indicating that some permanent damage had occurred.

The glass fiber shell effectively limited the oxidative damage to the CF core. This is an important issue, since the core is expected to carry more than 75% of applied loads. While oxygen diffused into the GF shell, penetration was limited to a few fiber diameters because the diffusion was coupled to a reaction process. Thus, oxygen never reached the CF/GF interface. Inspection of rods aged for 8736h showed no evidence of cracks or other damage. The only change observed was exfoliation of 1-2 fiber layers at the GF surface. The exfoliation of the surface layer can be attributed to structural changes in the matrix and shrinkage associated with the oxidation reaction, which left surface fibers exposed and un-bonded.

The extent of oxidation was limited, an assertion that was supported both by measurements and by model-based predictions of the TOLC for the composite rods. The self-arresting nature of the oxidation process suggests that the reaction product formed at the surface had a passivating effect on the oxidation reaction. The competition between the rate of oxygen diffusion and the rate of reaction between oxygen and the matrix determined the TOLC. The temperature dependence of the diffusion and reaction rates indicated that the ratio of the oxygen diffusion rate to the oxygen consumption rate decreased as the temperature increased. Consequently, the TOLC actually decreased with increasing aging temperature [25].

The oxygen concentration profiles provide some guidance for the design of hybrid composites for overhead conductors. The conductor design includes a GF shell to protect the CF core from galvanic corrosion and to limit thermal oxidation. The findings presented here allow one to estimate the required thickness of a GF shell to constitute an oxygen barrier. In particular, the TOLC was ~150 um, indicating that a safe design would include a shell substantially thicker than the thermal oxidation layer of the composite.

CONCLUSION

Accelerated aging studies were conducted on a hybrid GF/CF composite designed to support overhead power lines. The intent was to understand the moisture uptake and thermal oxidation mechanisms, and how they affect thermal and mechanical properties of the composite. The hybrid composite exhibited complex moisture absorption behavior that was attributed to the higher density packing of fibers located at the annular

GF/CF interface, which acted as a temporary moisture barrier. The GF shell dominated the diffusion rate for a significant portion of time, and as long as the concentration was less than the saturation level, SBS strength and T_g showed 77-98% retention after moisture removal. Sub-saturation levels of absorbed moisture caused only moderate damage to fiber-matrix interfaces because no cracks were observed microscopically, and the removal of moisture led to a significant recovery in thermal and mechanical properties [3].

A reaction-diffusion model was applied to the thermal oxidation of hybrid GF/CF composites to determine oxygen concentration profiles and the oxidized layer thickness. Model predictions were compared with experimental measurements of oxidized layer thickness, resulting in an accuracy of > 90% for up to a year of thermal exposure. The TOLC grew most during initial stages, and the growth rate decreased with increasing layer thickness, following parabolic kinetics. The layer did not grow appreciably after four days of exposure, and even exposures of one year at 180°C and 200°C caused no significant thickening. Thus, the oxidized surface layer effectively functioned as a passive layer, arresting the diffusion of oxygen and protecting the bulk epoxy from further oxidation. No evidence of cracking or other forms of damage was detected during long-term exposures up to one year. The crack resistance was attributed to the orientation of high-strength fibers parallel to the exposed surface. Strength retention of similar oxidized composites will depend in part on the ratio of the TOLC to the sample diameter. However, the strength loss is expected to be negligible in cases where the ratio of the TOLC to the sample diameter is small (<0.1).

An issue of practical importance for overhead conductors concerns the possible effect of thermal aging on long term durability and retention of mechanical properties. Although the oxidized surface layer reaches a self-limiting thickness and may protect the composite from progressive damage, the surface layer may be disrupted in service by phenomena such as abrasion from overlaid Al strands, cyclic bending loads, thermal cycles, and moisture absorption. Repeated disruption of the layer could undermine the protective effects and lead to progressive damage in service, although this possibility awaits further investigation. Finally, the effects of thermal aging may be more pronounced in small-diameter composite rods, in which the oxidized layer thickness constitutes a larger portion of the rod diameter.

ACKNOWLEDGEMENTS

The authors are grateful to Composite Technology Corporation for financial support.

References

1. A. Alawar, E.J. Bosze and S.R. Nutt, “A Composite Core Conductor for Low Sags and High Temperatures,” IEEE Trans. Power Delivery, 20 (3), p. 2193-99 (2005).
2. A. Alawar, E.J. Bosze, O. Bertschger, Yun-I Tsai and S. R. Nutt, “High-temperature Strength and Storage Modulus in Unidirectional Hybrid Composite,” Comp. Sci. Technol. 66, p. 1963-69 (2006).

3. Y-I Tsai, E.J. Bosze, and S.R. Nutt, “Influence of hygrothermal environment on thermal and mechanical properties of carbon fiber/fiberglass reinforced matrix composite materials,” Compos. Sci. Tech. 2008 **69** [3-4] (2009) 432-437 DOI.

4. Selzer R, Friedrich K., “Mechanical properties and failure behaviour of carbon fibre-reinforced polymer composites under the influence of moisture,” Composites A 1997;28:595–604.

5. Biro DA, Pleizer G, Deslandes Y., “Application of the microbond technique: effects of hydrothermal exposure on carbon-fiber/epoxy interfaces,” Compos. Sci. Tech. 1993;46:293–301.

6. Zhou J, Lucas JP., “The effects of a water environment on anomalous absorption behavior in graphite/epoxy composites,” Comp. Sci. Tech. 1995;53:57–64.

7. Ellyin F,Master R., “Environmental effects on the mechanical properties of glass fiber epoxy composite tubular specimens,” Comp. Sci. Tech. 2004;64:1863–74.

8. Imaz JJ, Rodrigurz JL, Rubio A, Mondragon I., “Hydrothermal environment influence on water diffusion and mechanical behaviour of carbon fiber/epoxy laminates,” J. Mater. Sci. Let 1991;20:662–5.

9. Wan YZ, Wang YL, Huang Y, He BM, Hah KY., “Hydrothermal aging behaviour of VARTMed three-dimensional braided carbon-epoxy composites under external stresses,” Composites A 2005;36:1102–9.

10. Shen CH, Springer GS. Moisture absorption of graphite–epoxy composites immersed in liquids and in humid air. J Comp Mater 1976;10:2–20.

11. Collings TA, Copley SM., “On the accelerated aging of CFRP,” Composites 1983;14:180–8. 406

12. Bullions TA, Loos AC, McGrath JE. “Moisture sorption effects and properties of a carbon fiber-reinforced phenylethynyl-terminated poly(etherimide),” J. Comp. Mater. 2003;37:791–809.

13. Luo HL, Lian JJ, Wan YZ, Huang Y, Wang YL, Jiang HJ., “Moisture absorption in VARTMed three-dimensional braided carbon–epoxy composites with different interface conditions,” Mater. Sci. and Eng. A 2006;425:70–7.

14. Thwe MM, Liao K., “Effects of environmental aging on the mechanical properties of bamboo–glass fiber reinforced polymer matrix hybrid composites,” Composites A 2002;33:43–52.

15. Wan YZ, Wang YL, Huang Y, Luo HL, He F, Chen GC., “Moisture absorption in three-dimensional braided carbon/Kevlar/epoxy hybrid composite for

orthopedic usage and its influence on mechanical performance," Composites A 2006;37:1480–4.

16. Lee MC, Peppas NA., "Water transport in graphite/epoxy composites," J. Appl. Polym. Sci. 1993;47:1349–59.

17. Loos AC, Springer GS., "Moisture absorption of graphite-epoxy composites immersed in liquids and in humid air," J. Comp. Mater. 1979;13:131–47.

18. Tsotsis T K., "Thermo-oxidative aging of composite materials," Journal of Composite Materials 1995. 29: p. 410-422.

19. Colin X, Verdu J., "Strategy for Studying Thermal Oxidation of Organic Matrix Composites," Composites Science and Technology 2005. 65: p. 411–419.

20. Bellenger V, Decelle J, Huet N., "Aging of a Carbon Epoxy Composite for Aeronautic Applications," Composite: Part B 2005. 36: p. 189-194.

21. Tsotsis. T K., "Long-term Thermo-oxidative Aging in Composite Materials: Experimental Methods," Journal of Composite Materials 1998. 58: p. 355–368.

22. Colin X, Marais C, Verdu J., "Thermal Oxidation Kinetics for a Poly(bismaleimide)," Journal of Applied Polymer Science 2001. 82: p. 3418–3430

23. Tandon G P, Pochiraju K V, Schoeppner G A., "Modeling of Oxidative Development in PMR-15 Resin," Polymer Degradation and Stability 2006. 91: p. 1861-1869.

24. Colin X, Marais C, Verdu J. "A New Method for Predicting the Thermal Oxidation of Thermoset Matrices Application to an Amine Crosslinked Epoxy," Polymer Testing 2001. 20: p. 795-803.

25. Le Huy H M, Bellenger V, Paris M, Verdu J., "Thermal Oxidation of Anhydride Cured Epoxies II. Depth Distribution of Oxidation Products," Polymer Degradation and Stability 1992. 35 p. 171-179.

26. Barjasteh E, Bosze E J, Nutt S R., "Thermal Oxidation of Anhydride Cured Epoxy and Epoxy Matrix Composites," Sampe 2008. 52, 12p.

27. Decelle J, Huet N, Bellenger V., "Oxidation Induced Shrinkage for Thermally Aged Epoxy Networks. Polymer Degradation and Stability," 2003. 81: p. 239–248.

28. Colin X, Mavel A, Marais C, Verdu J., "Interaction Between Cracking and Oxidation in Organic Matrix Composites," Journal of Composite Materials 2005. 39: p. 1371-1389.

29. Barjasteh E, Bosze E. J., Tsai Y.I., Nutt S R., "Thermal Aging of Fiberglass/Carbon fiber hybrid Composites," Compos. Sci. Tech. 2009 (in press).

30. Crank J., "The mathematics of diffusion," 2nd ed. p. 71–4. 429

31. Colin X, Marais C, J. Verdu J., "Kinetic Modelling of the Stabilizing Effect of Carbon Fibres on Thermal Ageing of Thermoset Matrix Composites," Composites Science and Technology 2005. 65 p. 117–127.

32. Wu Y S, Vliet J V, Frijlink H W, Maarschalk K V., "The Determination of Relative Path Length as a Measure for Tortuosity in Compacts Using Image Analysis," European Journal of Pharmaceutical Sciences 2006. 28: p. 433-440.

33. Matthews G P, Spearing M C., "Measurement and Modelling of Diffusion, Porosity and Other Pore Level Characteristics of Sandstones," Marine Petroleum Geology 1992. 9: p. 146-154.

34. Boyd J, Chang G, Webb W, Speak S., "Galvanic Corrosion Effects on Carbon Fiber Composites," In: 37th International SAMPE symposium and exhibition: materials working for you in the 21st century, 1992. 435: p. 1184–1198.